



# HHS Public Access

Author manuscript

*World J Pediatr Congenit Heart Surg.* Author manuscript; available in PMC 2018 November 28.

Published in final edited form as:

*World J Pediatr Congenit Heart Surg.* 2013 October ; 4(4): 362–366. doi:10.1177/2150135113501901.

## Bicuspid Aortic Valves Experience Increased Strain as Compared to Tricuspid Aortic Valves

Kai Szeto, BS<sup>1,2</sup>, Peter Pastuszko, MD<sup>3,4</sup>, Juan C. del Álamo, PhD<sup>2</sup>, Juan Lasheras, PhD<sup>2</sup>, and Vishal Nigam, MD<sup>1,5</sup>

<sup>1</sup>Department of Pediatrics (Cardiology), University of California San Diego, La Jolla, CA, USA

<sup>2</sup>Department of Mechanical Engineering, University of California San Diego, La Jolla, CA, USA

<sup>3</sup>Department of Surgery (Cardiothoracic Surgery), University of California San Diego, La Jolla, CA, USA

<sup>4</sup>Children's Mercy Hospital Kansas City, MO, USA

<sup>5</sup>Rady Children's Hospital Heart Institute San Diego, San Diego, CA, USA

### Abstract

**Objective:** To determine whether the leaflets of bicuspid aortic valve (BAV) experience increased strain when compared to tricuspid aortic valve (TAV) leaflets.

**Background:** The population at highest risk of aortic valve calcification (AVC) are individuals with BAVs. Currently, efforts to medically treat AVC are hampered by a limited understanding of the biomechanical forces involved in the molecular pathogenesis of AVC.

**Methods:** Surgically created BAVs and control TAVs were placed into a left heart simulator. Strains were calculated by comparing the distances between points on the aortic valve (AoV) leaflet during various time points during a simulated cardiac cycle.

**Results:** The fused leaflets of BAVs experience significantly more strain during systole when compared to TAVs. Specifically, BAVs experience 24% strain ( $P < .0001$ ) in the radial direction, parallel to the direction of blood flow, as compared to TAVs. There was peak difference of 4% ( $P < .001$ ) in the circumferential direction.

**Discussion:** Based upon the data presented here, we are in the process of identifying how increased strain activates calcification-associated pathways in AoV cells. Future studies will examine whether these stretch responsive pathways can be blocked to inhibit calcification of BAVs.

---

Reprints and permission: [sagepub.com/journalsPermissions.nav](http://sagepub.com/journalsPermissions.nav).

**Corresponding Author:** Vishal Nigam, Department of Pediatrics (Cardiology), University of California San Diego, 9500 Gilman Drive Box 0731, La Jolla, CA, USA. [vnigam@ucsd.edu](mailto:vnigam@ucsd.edu).

Declaration of Conflicting Interests

The author(s) declared no potential conflicts of interest with respect to the research, authorship, and/or publication of this article.

Supplemental Material

The online videos are available at <http://WJPCHS.sagepub.com/supplemental>.

## Keywords

aortic valve calcification; bicuspid aortic valve; mechanical stretch

---

## Introduction

Aortic valve calcification/stenosis (AVC) is the third leading cause of adult heart disease<sup>1</sup> and the most common form of acquired valvular disease in developed countries.<sup>2</sup> The risk factor most closely linked to calcific aortic stenosis is bicuspid aortic valve (BAV),<sup>2-5</sup> since 64% of the calcified aortic valves (AoVs) have BAV morphology.<sup>6</sup> Currently, the only treatment for severe AVC is replacement of the valve. Efforts to develop medical treatments for AVC have been hampered by a limited understanding of molecular mechanisms by which inflammatory and osteogenic pathways are activated in AVC.

The BAVs, the most common congenital heart defect with an incidence rate of 1% to 2%,<sup>2,4,5</sup> result from the failure of the aortic valve leaflets to separate during development. In BAVs, there is typically a fused aortic valve leaflet that is smaller than the two normal leaflets would have been. The other leaflet, the unfused leaflet, is typically of normal size. An *ex vivo* study of explanted BAVs from individuals who died from noncardiac causes suggests that the fused leaflet experiences significant stress.<sup>7</sup> This study did not quantify the biomechanical strains experienced by the fused leaflets nor compared them to the leaflets of a normal tricuspid aortic valve (TAV). Furthermore, attempts to quantify the changes in mechanical stretch experienced by BAVs and TAVs using computational models have been inconclusive.<sup>8</sup> Although much effort has been devoted to studying the role of the atherosclerotic processes in aortic valve (AoV) disease, there is evidence that aortic valve interstitial cells (AVICs) can calcify in a cell autonomous mechanisms.<sup>9-12</sup> Although there have been recent reports examining the role of altered shear stresses in the leaflets of BAVs,<sup>13-15</sup> very little is known about the strain experienced by BAVs. Elucidation of the hemodynamic forces imposed on the BAVs is important to the development of medical treatments for BAV calcific disease.

## Methods

### Quantification of Strain Experienced by BAVs and TAVs

Aortic valves were harvested from pigs sacrificed at the University of California San Diego Center for the Future of Surgery. The aortic valves and ascending aortic roots were mounted on Gore-Tex rings. To replicate the bicuspid AoV morphology, the left and right cusps were sutured together thereby replicating the most common valve morphology found in BAVs. For the purpose of quantifying the dynamic deformation and the resulting strain of the leaflets during the systolic phase of the cardiac cycle, we measured the relative displacement of small ink dots tattooed on the leaflets (each with an approximate diameter of 1 mm) during the opening phase of the valve. To maximize the resolution of the strain measurement, approximately 105 dots of an array of  $15 \times 7$  were marked on a single leaflet. The valves were mounted in a replica of the Georgia Tech Left Heart Simulator (Figure 1). A controlled programmable pulsatile pump was used to simulate the ejection of the heart's

left ventricle. In order to simulate physiological conditions of a normal cardiovascular system, the peak cardiac output and heart rate were 35 mL/s and 70 beats/min, respectively. In addition, the downstream compliance chamber and the resistance were calibrated to retain the physiological conditions of a human heart. A mixture of 60% of deionized water and 40% of ethylene glycol was used to simulate the viscosity of blood of approximately 4 cP.

High-resolution cameras were placed at different angles to record the location of the dots marked on the leaflets throughout the opening of the valves. Strain was calculated by quantifying the change in distance between the centers of dots in either the radial or the circumferential direction. A time point during diastole was used as the reference point. We then transformed pairs of two-dimensional (2D) images acquired at two different angles onto three-dimensional surfaces at each time point. Once the instantaneous shape of the leaflet was reconstructed, we compared the initial and final distance of the dots in both radial and circumferential directions. Strain was calculated by comparing the change in distance between the points at the systolic time point being examined to the reference divided by the distance between points at the reference point. Three valves were used to test each condition.

## Statistical Analysis

The statistical significance of differences between the groups was determined with the unpaired *t* test. *P* < .05 was considered significant. Standard error of the mean was calculated and included in the graphs.

## Results

The fused leaflet of BAVs experiences significantly more strain during systole. Given the lack of clarity regarding the relationship between valve morphology and the strain experienced by AoV leaflets, we performed *ex vivo* experiments using explanted porcine aortic valves. Based on the observation (Figure 2A and Supplemental video), the valves of both morphology closed and deformed in a similar manner at diastole. However, during systole, the BAVs deformed very differently than the TAVs most notably during peak systole. As a result of these observations, we focused on quantifying the strains experienced by the valves during systole. End diastole was used as the reference point, since TAVs and BAVs were similar at this time point. Although there was a statistically significant difference (*P* = .001), the magnitude of the peak strains in circumferential direction was very similar between the BAVs (14%) and the TAVs (10%). During mid-to-late systole, the fused valve leaflets of BAVs experienced a significantly higher peak strain of 24% in the radial stretching when fully open as compared to the peak of 4% in the TAV (*P* < .0001 at the measured time points; Figure 2D and Table 1).

## Discussion

In this report, we demonstrate that BAV leaflets experience significantly more radial strain during systole as compared to TAVs. This is the first report experimentally comparing the strains experienced by BAVs as compared to TAVs during systole. We have focused on the strain imposed on BAV leaflets, since strain is of much greater magnitude than shear stress.

Additionally, the strain directly affects AVICs, which are the cells that calcify in AVC. Previously, Robicsek et al examined the strain experienced by explanted human BAVs; however, they did not compare the differences between BAVs and TAVs.<sup>7</sup> On the other hand, computer modeling predicted minimal changes in the forces experienced by leaflets in TAVs and BAVs.<sup>8</sup> Our data demonstrate that the fused leaflets of BAVs experience significantly more strain in the radial direction than TAV leaflets. One possible explanation for the difference between the experimental data and the *in silico*<sup>8</sup> data is that the *in silico* BAVs were modeled as having symmetric valve leaflets instead of the morphology seen in patients in which the fused leaflet is larger than the unfused one. A limitation of our study is that we used surgically created porcine BAVs. This approach was necessary since large animals with BAVs and noncalcified human BAVs were not available. Based upon our data, we believe that the fused leaflets of BAVs experience significantly more strain than the leaflets in normal TAVs. Additionally, we propose that the patients with BAVs that experience increased strain will be the subset of developing AVC. Future efforts to noninvasively measure the valve leaflet strains would be a powerful tool for risk stratification patients with BAV for their potential of developing significant AVC.

It has been reported that cultured aortic valve, AVICs exposed to cyclic stretch have an increased expression of genes associated with AVC.<sup>16,17</sup> In separate reports, we are in the process of describing the discovery that stretch-mediated repression of a microRNA and a long noncoding RNA are critical to the increased expression of calcification-associated genes in human AVICs. We have previously demonstrated that microRNAs are altered in BAVs.<sup>18</sup> Based upon the data presented here and the aforementioned molecular data from our laboratory, we have developed the model that stretch activation of calcification-associated genes in response to the increased strain imposed on AVICs in BAVs is sufficient to cause AVC (Figure 3). This model will serve as a roadmap to identifying stretch responsive pathways that can be targeted to prevent calcification of BAVs. Ongoing efforts to elucidate the role that biomechanical stimuli plays in the pathogenesis of calcific disease of BAVs are important development of noninvasive treatments for this serious disease.

## Supplementary Material

Refer to Web version on PubMed Central for supplementary material.

## Acknowledgment

The authors would like to thank the Center for the Future of Surgery at University of California San Diego for their assistance in obtaining the porcine aortic valves.

### Funding

The author(s) disclosed receipt of the following financial support for the research, authorship and/or publication of this article: VN was supported by NIH K08 HL086775-01.

## Abbreviations and Acronyms

<b>BAV</b>	bicuspid aortic valve
<b>AoV</b>	aortic valve

<b>AVC</b>	aortic valve calcification
<b>TAV</b>	tricuspid aortic valve
<b>AVICs</b>	aortic valve interstitial cells

## References

1. Association AH. Heart Disease and Stroke Statistics—2004 Update. American Heart Association: Dallas, TX; 2004.
2. Freeman RV, Otto CM. Spectrum of calcific aortic valve disease: pathogenesis, disease progression, and treatment strategies. *Circulation*. 2005;111(24): 3316–3326. [PubMed: 15967862]
3. Ward C. Clinical significance of the bicuspid aortic valve. *Heart*. 2000;83(1): 81–85. [PubMed: 10618341]
4. Fedak PW, Verma S, David TE, Leask RL, Weisel RD, Butany J. Clinical and pathophysiological implications of a bicuspid aortic valve. *Circulation*. 2002;106(8): 900–904. [PubMed: 12186790]
5. Beppu S, Suzuki S, Matsuda H, Ohmori F, Nagata S, Miyatake K. Rapidity of progression of aortic stenosis in patients with congenital bicuspid aortic valves. *Am J Cardiol* 1993;71(4): 322–327. [PubMed: 8427176]
6. Davies MJ, Treasure T, Parker DJ. Demographic characteristics of patients undergoing aortic valve replacement for stenosis: relation to valve morphology. *Heart*. 1996;75(2): 174–178. [PubMed: 8673757]
7. Robicsek F, Thubrikar MJ, Cook JW, Fowler B. The congenitally bicuspid aortic valve: how does it function? Why does it fail? *Ann Thorac Surg* 2004;77(1): 177–185. [PubMed: 14726058]
8. Weinberg EJ, Shahmirzadi D, Mofrad MR. On the multiscale modeling of heart valve biomechanics in health and disease. *Biomech Model Mechanobiol* 2010;9(4): 373–387. [PubMed: 20066464]
9. Mohler ER, III, Chawla MK, Chang AW, et al. Identification and characterization of calcifying valve cells from human and canine aortic valves. *J Heart Valve Dis* 1999;8(3): 254–260. [PubMed: 10399657]
10. Rajamannan NM, Subramaniam M, Rickard D, et al. Human aortic valve calcification is associated with an osteoblast phenotype. *Circulation*. 2003;107(17): 2181–2184. [PubMed: 12719282]
11. Jian B, Jones PL, Li Q, Mohler ER, III, Schoen FJ, Levy RJ. Matrix metalloproteinase-2 is associated with tenascin-C in calcific aortic stenosis. *Am J Pathol* 2001;159(1): 321–327. [PubMed: 11438479]
12. Clark-Greuel JN, Connolly JM, Sorichillo E, et al. Transforming growth factor-beta1 mechanisms in aortic valve calcification: increased alkaline phosphatase and related events. *Ann Thorac Surg* 2007;83(3): 946–953. [PubMed: 17307438]
13. Saikrishnan N, Yap CH, Milligan NC, Vasilyev NV, Yoganathan AP. In vitro characterization of bicuspid aortic valve hemodynamics using particle image velocimetry. *Ann Biomed Eng* 2012; 40(8): 1760–1775. [PubMed: 22318396]
14. Yap CH, Saikrishnan N, Tamilselvan G, Vasilyev N, Yoganathan AP. The congenital bicuspid aortic valve can experience high-frequency unsteady shear stresses on its leaflet surface. *Am J Physiol Heart Circ Physiol* 2012;303: H721–H731. [PubMed: 22821994]
15. Sun L, Chandra S, Sucusky P. Ex vivo evidence for the contribution of hemodynamic shear stress abnormalities to the early pathogenesis of calcific bicuspid aortic valve disease. *PLoS ONE*. 2012;7(10): e48843. [PubMed: 23119099]
16. Balachandran K, Sucusky P, Jo H, Yoganathan AP. Elevated cyclic stretch alters matrix remodeling in aortic valve cusps: implications for degenerative aortic valve disease. *Am J Physiol Heart Circ Physiol* 2009;296(3): H756–H764. [PubMed: 19151254]
17. Lehmann S, Walther T, Kempfert J, et al. Mechanical strain and the aortic valve: influence on fibroblasts, extracellular matrix, and potential stenosis. *Ann Thorac Surg* 2009;88(5): 1476–1483. [PubMed: 19853097]

18. Nigam V, Sievers H, Jensen B, et al. Altered microRNAs in bicuspid aortic valves: a comparison between stenotic and insufficient valves. *J Heart Valve Disease*. 2010;19(4): 459–465. [PubMed: 20845893]

Author Manuscript

Author Manuscript

Author Manuscript

Author Manuscript

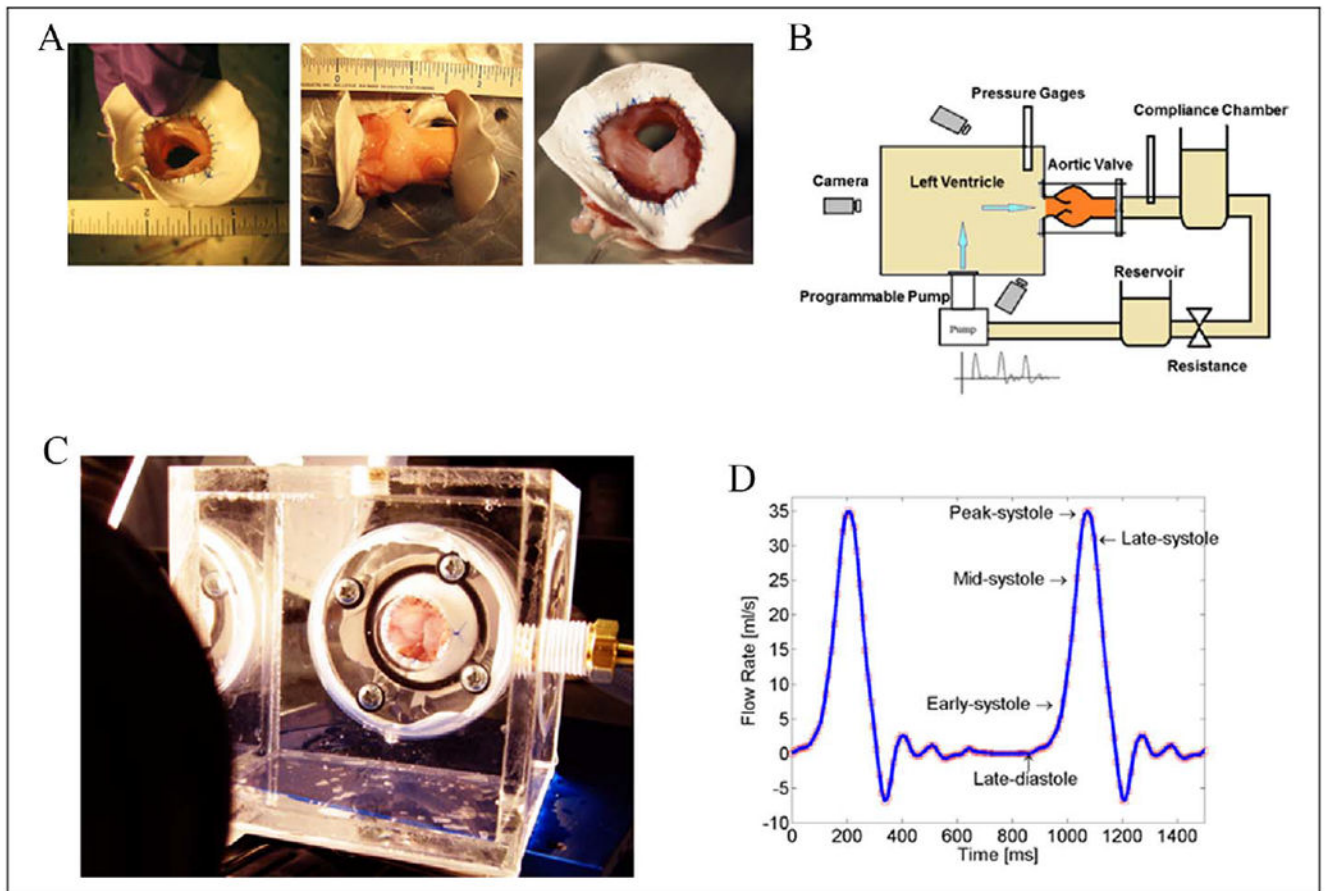


**Figure 1.**

Experimental design. A, Pictures of aortic valves sutured to the Gore-Tex rings. The right picture is a bicuspid aortic valve (BAV). B, Diagram of the left heart simulator used. C, Picture of the clear left ventricle stimulator used. D, Tracing of the flow pattern used to stimulate the blood flow through the aortic valve.

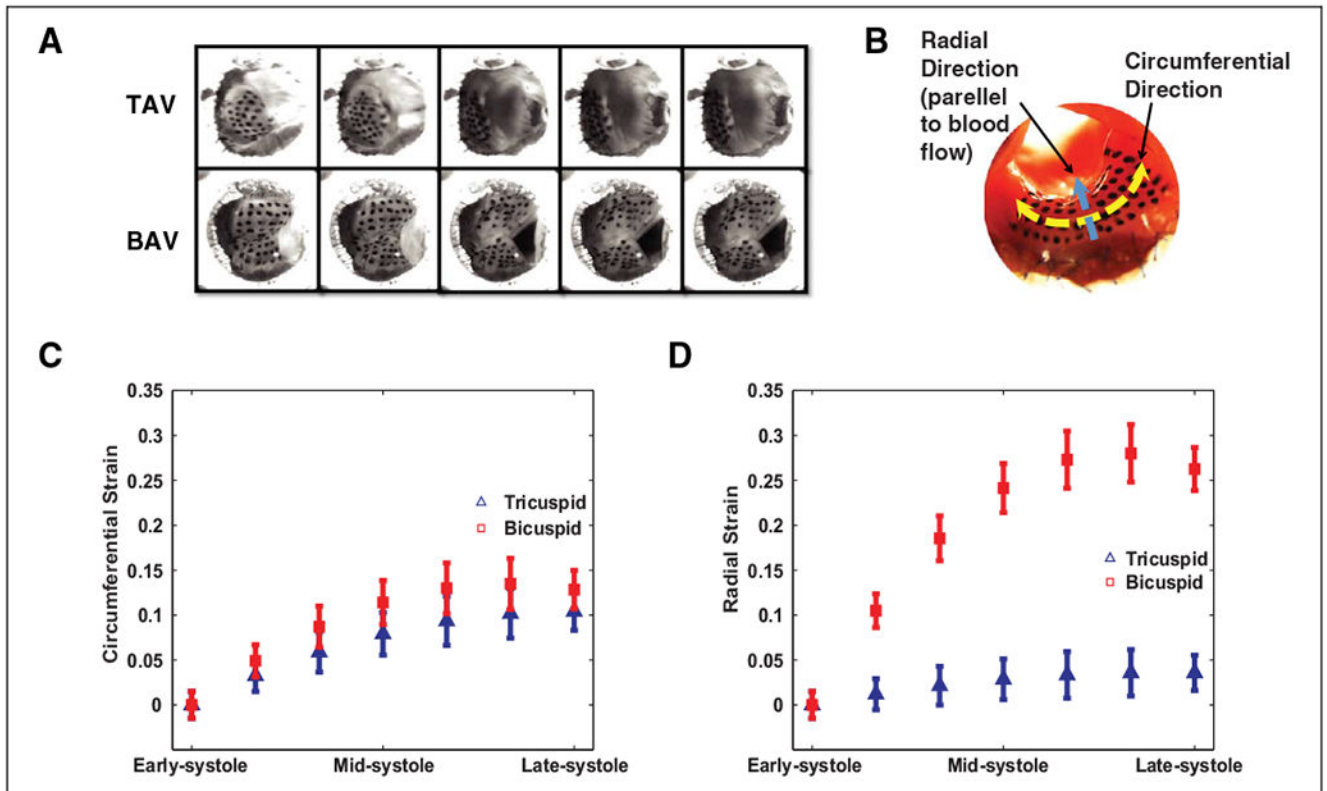


**Figure 2.**

Bicuspid aortic valves (BAVs) experience significantly more strain during systole. A, Still frames of the aortic valve leaflets during the cardiac cycle. The left frames are at diastole (the reference point). The right images are at peak systole. B, An image of a tricuspid aortic valve (TAV) with the ink dots on the ventricular side of the aortic valve (AoV) leaflet. The blue arrow demarcates the radial direction (parallel to blood flow). Radial direction is parallel to blood flow while the circumferential direction parallel to the aortic valve annulus plane. C, There is a 4% increase in the strain of BAV in the circumferential as compared to the TAV. D, The BAVs experience peak difference of 24% more strain in the radial direction as compared to the TAVs.  $N=3$  different valves for each group.



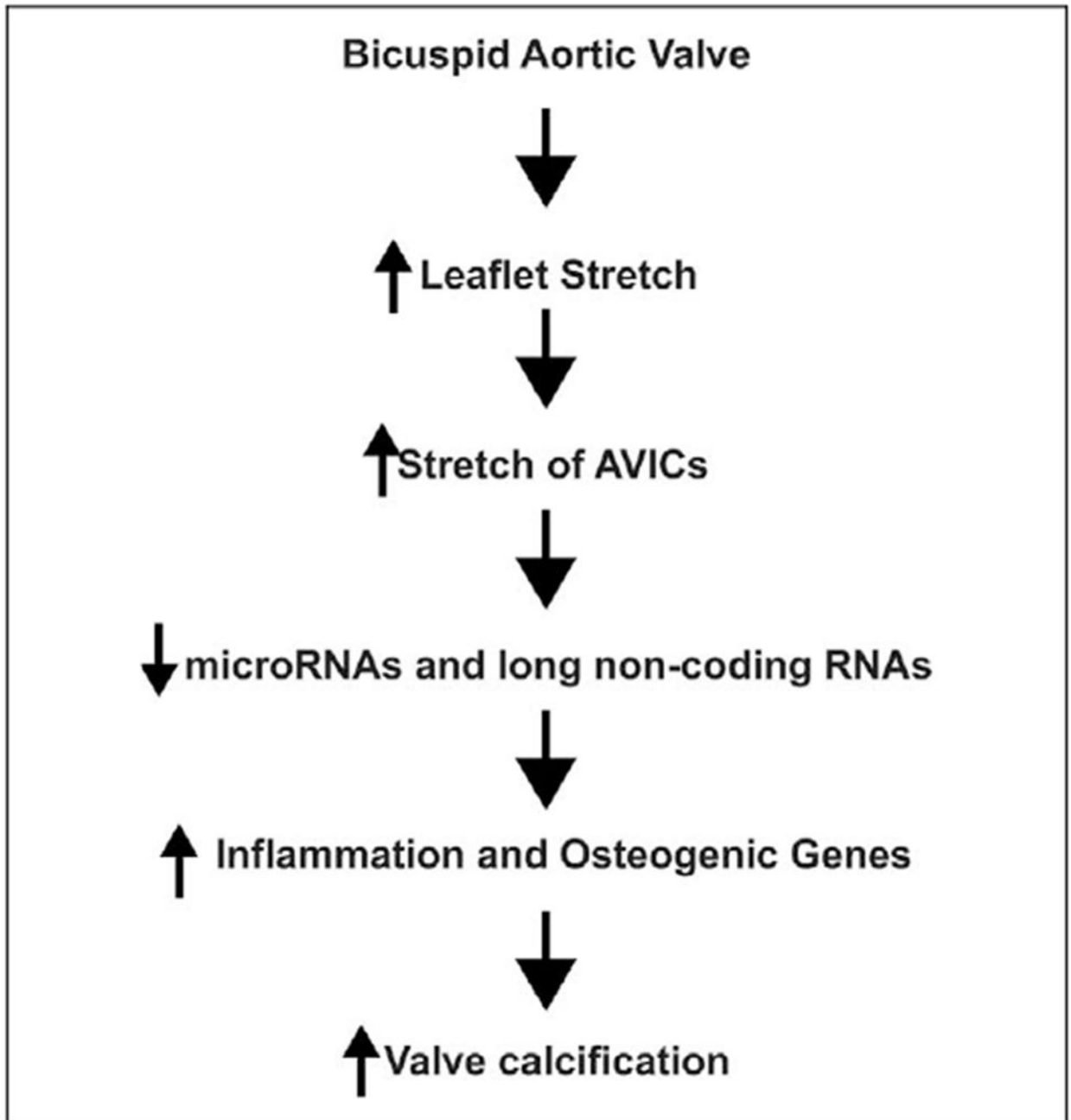


**Figure 3.** Model of how biomechanical stretch activate calcification related pathways in bicuspid aortic valves (BAVs).

Quantification of Stretch. Average stretch values were computed at 6 different time points from early systole to late systole in both radial and circumferential direction. Stretch values were computed as the changes of distance of distance of dots divided by the distance of reference. N = 3 different valves for each group.

**Table 1.**

	(Reference Point)	Mid Systole	Late Systole
Radial stretch data (in unit of 100%)			
Tricuspid valves stretch			
Mean value	1.00	1.033	1.032
Standard deviation (±)	0.013	0.024	0.023
Bicuspid valves stretch			
Mean value	1.113	1.233	1.275
Standard deviation (±)	0.02	0.03	0.03
P values	<.0001	<.0001	<.0001
Circumferential stretch data (in unit of 100%)			
Tricuspid valves stretch			
Mean value	1	1.092	1.099
Standard deviation (±)	0.019	0.023	0.013
Bicuspid valves stretch			
Mean value	1	1.111	1.13
Standard deviation (±)	0.012	0.017	0.013
P values	.011	.032	.001